Effects of Atmospherically Important Solvated Ions on Organic Acid Adsorption at the Surface of Aqueous Solutions

Melissa C. Kido Soule, Patrick G. Blower, and Geraldine L. Richmond*

Department of Chemistry, University of Oregon, 1253 University of Oregon, Eugene, Oregon 97403

Received: June 26, 2007; In Final Form: September 18, 2007

The effects of salts on the solubility of amphiphilic organic molecules are of importance to numerous atmospheric, environmental, and biological systems. A detailed picture of the influence of dissolved atmospheric salts, NaCl and Na_2SO_4, on the adsorption of hexanoic acid at the vapor/water interface is developed using vibrational sum-frequency spectroscopy and surface tension measurements as a function of time, organic concentration, and solution pH. We have found that for hexanoic acid adsorption at the vapor/water interface, a fast initial adsorption is followed by two considerably slower processes: a reorientation of the polar headgroup and a restructuring of the headgroup solvation shell. The addition of salts affects this restructuring by reducing the range of water−headgroup interactions immediately upon surface adsorption for ion containing solutions. Reorientation of the organic headgroup with time occurs at the surface of both salt-containing and salt-free solutions, but the most stable orientation differs with the added ions. The dissolved salts also enhance the interfacial concentration of hexanoic acid, consistent with the known salting-out behavior of Cl^- and SO_4^{2-} anions.

1. Introduction

There is an increasing appreciation for the influence of dissolved ions on the aqueous surface adsorption of organic amphiphilic compounds. In biological systems, the adhesion and adsorption of cells, proteins, and small molecules at interfaces with water occur in the presence of fairly high concentrations of salts.[1] In the atmosphere, growing evidence for organic molecules adsorbed at aerosol surfaces has led to much interest in their role in aerosol chemistry. In addition to inorganic chemical species, aerosol particles can have a large organic content, up to 50% of the aerosol mass depending on location.[2−5] Of this, carboxylic acids that partition to the air/water interface are among the most abundant.[6,7] The presence of organic films has been shown to influence the ability of aerosols to absorb water vapor and to nucleate clouds, and consequently, can significantly affect their role in regulating Earth's climate.[5,8] The presence of organic material at aerosol surfaces has also been shown to affect their absorptive and chemical properties. In one study, a near monolayer coverage of hexanoic acid at an artificial seawater aerosol surface decreased the uptake of N_2O_5 by a factor of 3 or 4.[8] This result is of interest because heterogeneous reactions of N_2O_5 on aerosol surfaces are important mechanisms for nitrogen oxide radical (NO_x) loss and a source of Cl radical in the atmosphere. Given the central role that aerosol particles play in atmospheric chemistry and in regulating the climate, it is important to understand how dissolved ions influence the microscopic composition and structure of organic species adsorbed at the surface of salt-rich aerosols.

Equilibrium surface tension measurements indicate that the presence of NaCl and $(NH_4)_2SO_4$ results in an enhancement of the adsorption of a soluble *n*-alkanoic acid, hexanoic acid, at the air/water interface.[9] These thermodynamic measurements alone, however, cannot provide molecular-level insight into what factors are responsible for this enhanced organic surface adsorption. Such microscopic information can be provided by vibrational sum-frequency spectroscopy (VSFS), which is sensitive to molecules in the top layers of the water surface.[10−12] As a second-order nonlinear technique, it is inherently surface-selective because of the break in inversion symmetry at interfaces and can be used to determine surface structure, chemical identity, and molecular orientation in the interfacial region.

In this study, we use VSFS to investigate the molecular-level effects of salts on the adsorption behavior of organic molecules at an aqueous interface. To model the organic−inorganic aerosol surface, we have chosen organic and inorganic species that are found in the atmosphere. Specifically, we compare the adsorption of hexanoic acid at the air/water interface in the absence and presence of NaCl and Na_2SO_4. Sum-frequency and surface tension measurements are made as a function of time to elucidate the effects of high salt concentration on the adsorption dynamics. Spectroscopic measurements as a function of pH are also used to deconvolute the effects of pH and ionic strength on the organic adsorption.

Vibrational sum-frequency spectroscopy is described extensively in the literature and so only a brief summary is given here.[11−13] In VSFS, a tunable infrared pulse (ω_{IR}) is overlapped with a fixed-frequency visible pulse (ω_{vis}) spatially and temporally at an interface between two centrosymmetric media to generate signal at the sum of the incident frequencies, $\omega_{SF} = \omega_{IR} + \omega_{vis}$. The sum-frequency signal intensity is proportional to the intensities of the incident beams and to the square of the effective second-order susceptibility, $\chi^{(2)}_{eff}$, which is in turn related to the true second-order susceptibility by Fresnel factors and unit polarization vectors for each beam.

$$I(\omega_{SF}) \propto |\chi^{(2)}_{eff}|^2 I(\omega_{vis}) I(\omega_{IR}) \quad (1)$$

* Author to whom correspondence should be addressed. E-mail: richmond@uoregon.edu. Phone: 541-346-4635. Fax: 541-346-5859.

10.1021/jp074986b CCC: $37.00
Published on Web 11/16/2007

The second-order susceptibility $\chi^{(2)}$ can be expressed as the sum of a nonresonant component, $\chi^{(2)}_{NR}$, and a resonant component for each vibrational mode ν, $\chi^{(2)}_{R_\nu}$.

$$\chi^{(2)} = \chi^{(2)}_{NR} + \sum_{\nu} \chi^{(2)}_{R_\nu} \quad (2)$$

In general, both $\chi^{(2)}_{NR}$ and $\chi^{(2)}_{R\nu}$ are complex quantities. In these studies, we assume that ω_{vis} is far enough from any electronic transitions and therefore that the nonresonant component is real. The resonant susceptibility, $\chi^{(2)}_R$, is related to the molecular hyperpolarizability, β, through the number density of probed molecules, N, and their orientation:

$$\chi^{(2)}_R = \frac{N}{\epsilon_o}\langle\beta\rangle \quad (3)$$

where the angular brackets denote an ensemble average over all possible molecular orientations.

The intensity of the sum-frequency signal depends on several factors including the number density in the interfacial region, the molecular orientation, and the vibrational mode transition strength. The VSFS signal is also polarization dependent. Probing the nonzero elements of $\chi^{(2)}_{ijk}$ with different combinations of polarized light can help to isolate these effects on the sum-frequency spectrum. All data in this work were recorded in ssp and sps polarization combinations, which probe the $\chi^{(2)}_{yyz}$ and $\chi^{(2)}_{yzy}$ elements of the second-order susceptibility, respectively. The polarizations schemes are given in the format: sum-frequency, visible, infrared.

2. Experimental Section

Spectroscopic Measurements. The sum-frequency spectra discussed here were obtained using a broad-bandwidth sum-frequency generation laser system. The experimental setup, described elsewhere,[14] is detailed briefly here. The ~100 fs output of a Ti:Sapphire laser at 800 nm is amplified and split, with approximately 15% of the output used to produce ~2 ps pulses directed to the interface. The remaining output is used in an optical parametric amplifier (OPA) where tunable infrared light from 3 to 10 μm is produced. In the present studies, the OPA was tuned to the C═O stretching region near 1700 cm^{-1} where the IR energy was typically 6 μJ per pulse with 175 cm^{-1} bandwidth. The IR beam was entirely enclosed in a box containing an overpressure of dry air, which reduced IR losses due to adsorption by water vapor in this wavelength region. The experiments were conducted in external reflection geometry, and the generated sum-frequency light was collected with a spectrometer and a liquid nitrogen cooled CCD camera. The ssp-polarization spectra here were obtained during 5 min CCD acquisitions, while the sps-polarization spectra were obtained during 10 min acquisitions. Spectra were normalized with the nonresonant VSFS spectrum from an amorphous gold surface, and calibrated using the narrow features in the gold spectrum because of water vapor absorption. The error in calibrating the IR frequency is ± 2 cm^{-1}.

The broad-bandwidth nature of the BBSFG method allows for the acquisition of an entire vibrational spectrum with a single laser pulse and consequently can considerably shorten spectral acquisition times and enable the observation of surface dynamics. Sum-frequency spectra are presented here in which a sample surface was interrogated within ~5−10 min after initial sample preparation. Several successive 5 min (ssp polarization) or 10 min (sps polarization) spectra were taken daily to document reproducibility and sample stability. No differences were observed between the successive spectra over this ~30 min period, and thus they were averaged to produce the spectra referenced here as $t = 0$. Spectra are also presented in which the sample was interrogated again ~1−1.5 h after initial sample preparation. Again, successive spectra taken over ~30 min showed no significant differences and were thus averaged to give the spectrum referenced here as $t = 1.5$ h. However, significant changes were observed between the averaged $t = 0$ and the $t = 1.5$ h spectra for certain hexanoic acid solutions. These dynamic changes at the sample surface occur between approximately 30 min and 1−1.5 h after the initial sample preparation. All experiments were performed at room temperature.

Because the VSFS intensity is related to the squared coherent sum of the non-resonant and resonant susceptibility components, interferences may occur that lead to distortions in peak shape and apparent peak frequency. To accurately interpret the data, VSFS spectra are fit to a line shape that accounts for the effects of homogeneous broadening (Lorentzian line shape) and inhomogeneous broadening (Gaussian line shape).[15−17]

$$|\chi^{(2)}(\omega_{SF})|^{(2)} = \left|\chi^{(2)}_{NR} + \int_{-\infty}^{\infty} \frac{A_\nu}{\omega_L - \omega_{IR} - i\Gamma_L} \exp\left[-\frac{(\omega_L - \omega_\nu)^2}{\Gamma_\nu^2}\right] d\omega_L\right|^2 \quad (4)$$

In this expression A_ν is the resonant amplitude, ω_ν is the resonant frequency, and Γ_L and Γ_ν are the homogeneous and inhomogeneous line widths. Each of the resonant terms and the non-resonant term has a unique phase associated with it. For the spectral analyses here, the Lorentzian width was set to 2 cm^{-1} and the nonresonant background was constrained to be real and negative. Our global fitting analysis includes a series of tightly held constraints on the peak phases, widths, and locations obtained from spectra recorded in different (yet related) environments. In this way, a more rigorous analytical fit to the data is achieved with curve parameters that are consistent across the series of spectra.

Surface Tension. All surface tension measurements were made at 25 °C using the Wilhelmy plate method with a KSV Instruments tensiometer.[18,19] For these samples, a thin glass microscope coverslip was used to minimize organic adhesion.[20] The glass plate was made hydrophilic by soaking overnight in piranha solution (2:1, H_2SO_4:H_2O_2), rinsed with Nanopure water, and dried before use. For the hexanoic acid measurements, each solution was injected into a glass sample dish, and 1−2 min elapsed before the surface tension was recorded. In the dynamic studies, the surface tension was continuously monitored for 120 ± 5 min. The typical resolution of the recorded surface tension was ±0.5 mN/m. Before each experimental run, the surface tension of pure water was measured and was consistently found to be in agreement with the literature value for water at the above temperature.

Sample Preparation. Hexanoic acid (Sigma-Aldrich, 99.5%+), NaCl (Fluka, 99.5%+), and Na_2SO_4 (Sigma-Aldrich, 99%+) were used as received without further purification. Aqueous solutions were prepared using water from an 18 MΩ Nanopure system. Samples were placed in a custom-designed cell made of KEL-F with CaF_2 input and BK-7 output windows and sealed with VITON O-rings. The sample cell and all glassware were cleaned with a H_2SO_4/NOCHROMIX solution followed by copious rinses with Nanopure water.

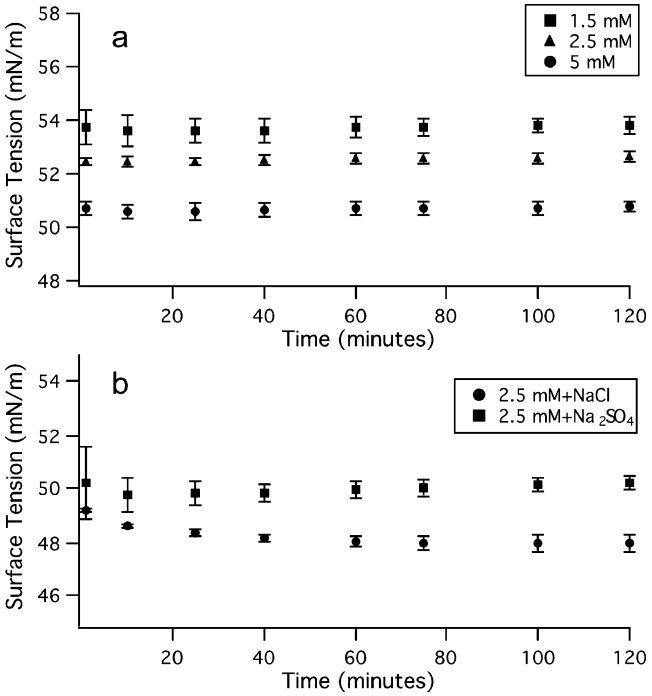

Figure 1. Surface tension γ for aqueous solutions of hexanoic acid measured as a function of time at 25 °C degrees for (a) 1.5, 2.5, and 5 mM concentrations, and for (b) 2.5 mM hexanoic with 3 M NaCl and 1 M Na_2SO_4.

3. Results and Discussion

The results of surface tension measurements as a function of time for select concentrations of hexanoic acid with and without added salts are presented first. The presentation and discussion of VSFS spectra of hexanoic acid at the air/water interface in ssp and sps polarizations follows, in which the molecular structure of the surface adsorbed organic is compared at different time intervals following initial injection of the solution. The effects of added salts on the organic adsorption are presented last and are compared with the adsorption behavior observed at the salt-free aqueous interface.

Surface Tension. Surface tension measurements as a function of time were conducted for hexanoic acid at the surface of solutions with and without salts to provide complementary information to the spectral data. The adsorption kinetics of hexanoic acid at short times (surface lifetimes <20 ms) have been reported in the literature.[21,22] However, because we have found that the VSFS spectra change in a longer time frame following initial sample preparation, we focus here on surface tension changes over the longer time frame.

The traces in Figure 1a show the surface tension−time dependence of 1.5, 2.5, and 5 mM solutions of hexanoic acid. Data were recorded from ∼2 min to a few hours after the sample was injected into the sample dish. The surface tensions were compared with those for hexanoic acid in the literature and found to be in reasonable agreement.[9] The data show that the surface tension at each organic concentration does not change within experimental certainty between the initial measurement and that recorded over 1.5 h later. Likewise, the surface tension−time traces in Figure 1b for hexanoic acid solutions with NaCl and Na_2SO_4 are also essentially constant. The constant nature of the surface tension at long time in Figure 1 shows that organic adsorption at the air/water interface is essentially immediate on the time scale here and that no additional adsorption at surfaces with or without added salts occurs over an extended equilibration period.

Surface tension measurements as a function of hexanoic acid concentration were also made for hexanoic solutions without salt and with 3 M NaCl and 1 M Na_2SO_4. The surface pressure isotherms for these solutions are shown in Figure 2a, and as

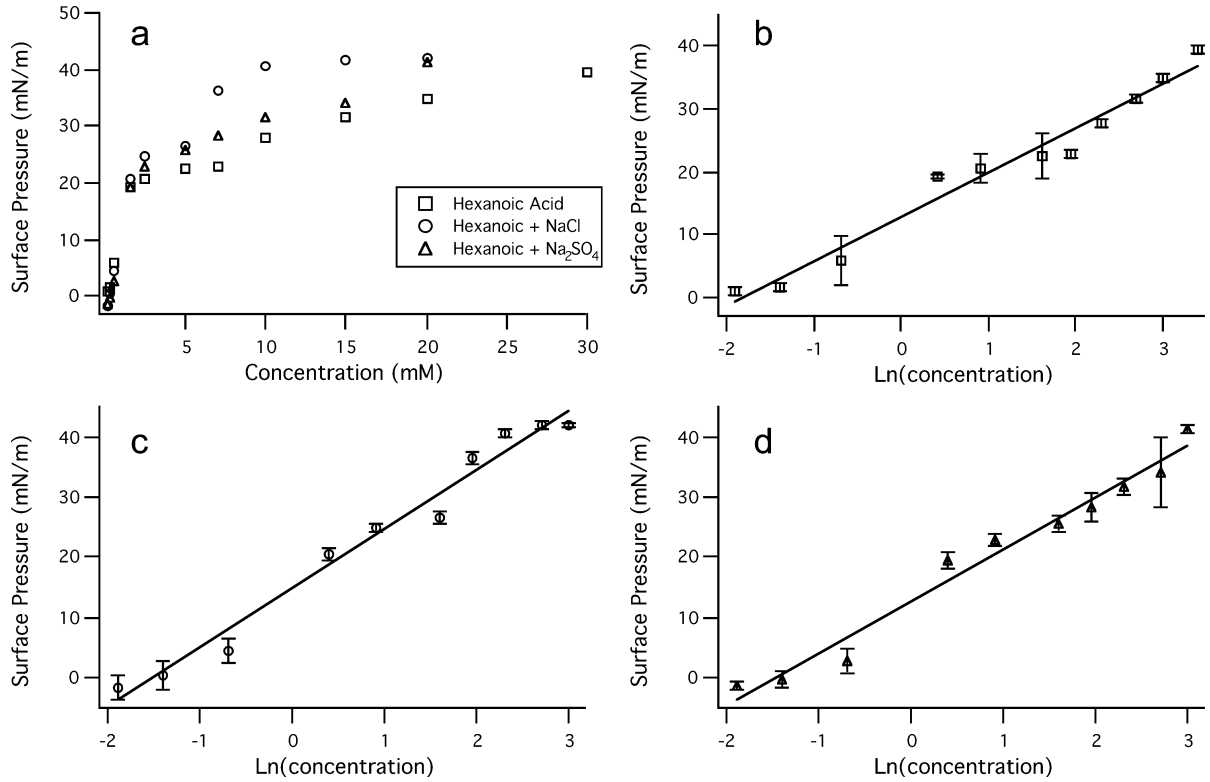

Figure 2. (a) Surface pressure isotherms for hexanoic acid at the air/water interface, and at hexanoic acid solution interfaces containing 3 M NaCl and 1 M Na_2SO_4. Surface pressure data as a function of the natural log of organic concentration for (b) hexanoic acid without added salt, (c) hexanoic acid with NaCl, and (d) hexanoic acid with Na_2SO_4 are fit to the Gibbs equation (solid line).

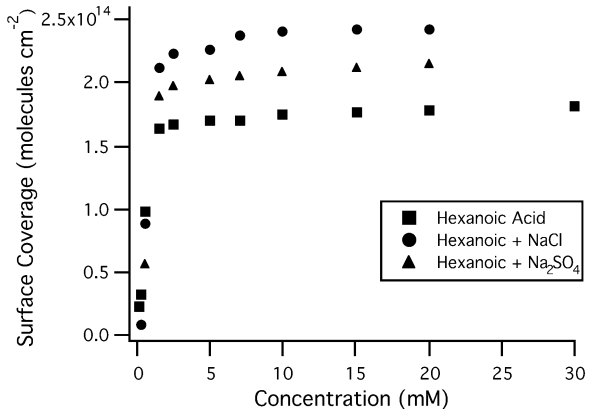

Figure 3. Surface coverage of hexanoic acid as a function of acid concentration for solutions without added salt, with 3 M NaCl, and with 1 M Na_2SO_4.

expected, the surface pressure increases with increasing organic concentration. The surface pressure values are also generally higher upon addition of both NaCl and Na_2SO_4 to the hexanoic acid solutions, although the pressure increase is more significant with NaCl. To determine the limiting organic surface concentration, the surface pressure isotherms in Figure 2a are fit to the Gibbs equation:[23]

$$\Gamma_i = \frac{1}{RT}\left(\frac{\partial \pi}{\partial \ln a_i}\right)_T \tag{5}$$

where Γ_i is the surface excess concentration at maximum surface coverage, π is the interfacial pressure in mN/m, and a_i is the activity. For the dilute hexanoic solutions here, the activity is replaced by the bulk concentration. Figure 2b−d shows the surface pressure data recast in the form of the Gibbs equation (pressure vs natural log of concentration). A linear fit to the data yields the limiting surface excess for each hexanoic acid solution.

The surface coverage at any bulk concentration is then obtained from Γ_i and the Frumkin equation:[23]

$$\pi_2 = -\Gamma_i \ln\left[1 - \frac{\Gamma_2}{\Gamma_i}\right] \tag{6}$$

where the subscript 2 indicates the surface pressure or surface excess at a specific bulk concentration. Hexanoic acid surface coverage data are shown in Figure 3 as a function of organic concentration. These results show that the surface coverage of hexanoic acid is higher in the presence of ions for organic concentrations above 0.5 mM. The magnitude of this surface adsorption enhancement is greater for solutions with 3 M NaCl than with 1 M Na_2SO_4.

VSFS Spectra of Hexanoic Acid Adsorption at the Air/Water Interface. VSFS spectra taken under ssp and sps polarizations of the freshly prepared ($t = 0$) vapor/hexanoic acid solution interface are shown in Figure 4 for several acid bulk concentrations. Only one feature is seen in the spectra corresponding to the symmetric stretch of the C═O group of the undissociated acid. The concentration series were fit globally using eq 4 with a nonresonant background and single resonant component. The fits to the data in Figure 4 were achieved by constraining the C═O peak position to be equal for all spectra, while the resonant phases and Gaussian peak widths were held constant across the concentrations but allowed to vary between polarization schemes. The result is an excellent fit for both sets of data using these spectral constraints. The slight peak

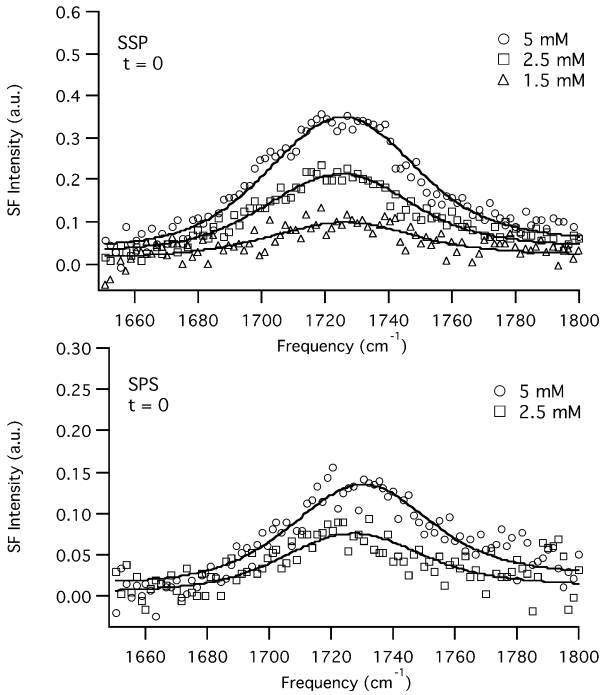

Figure 4. VSFS spectra of the C═O stretching vibration of hexanoic acid at the freshly prepared ($t = 0$) solution surface for different bulk concentrations. VSFS spectra are shown under the ssp (top, 5 min acquisition time) and sps (bottom, 10 min acquisition time) polarization combinations. Smooth lines are fits to the data.

asymmetry evident in Figure 4 is indicative of interference between the resonant and nonresonant components of $\chi^{(2)}$. The average peak widths and amplitudes obtained from fitting are shown with their corresponding uncertainties in Table 1 for these and other hexanoic acid solutions examined in this study.

VSFS intensity in the C═O region in Figure 4 increases monotonically in the ssp spectra as the bulk concentration of hexanoic acid increases between 1.5 and 5 mM and increases in the sps spectra between 2.5 and 5 mM. This trend in the $t = 0$ sum-frequency spectra is due to differences either in the hexanoic acid surface number density, in adsorption leading to different molecular orientations of the surface hexanoic acid, or to both. If the acid headgroup orientation at the surface varies for different bulk concentrations, then the sps/ssp ratio of peak amplitudes for the different concentrations should reflect this change. However, spectral fitting shows that this ratio is the same within experimental uncertainty for 2.5 mM (0.57 ± 0.06) and 5 mM (0.61 ± 0.04). This indicates that the headgroup orientation is invariant with changes in bulk concentration. We conclude that the spectral intensity increase in Figure 4 is primarily due to higher concentrations of hexanoic acid at the surface as the bulk concentration increases. A plot of the C═O spectral amplitude against the number density of molecules at the interface in Figure 5 verifies this conclusion. Since the sum-frequency intensity depends on both the surface number density and the molecular orientation, this plot will be linear if the VSFS amplitude correlates directly with surface coverage and will be nonlinear if the average orientation is also changing with surface coverage. The linear relationship shown in Figure 5 demonstrates that the increases in spectral intensity in Figure 4 can be attributed to one dominant factor, an increase in surface adsorption with bulk hexanoic acid concentration.

Spectral fitting places the C═O stretching frequency for hexanoic acid at the air/water interface at 1720 ± 2 cm^{-1} for all concentrations in Figure 4. The well-known sensitivity of the frequency of this mode to solvent environment provides

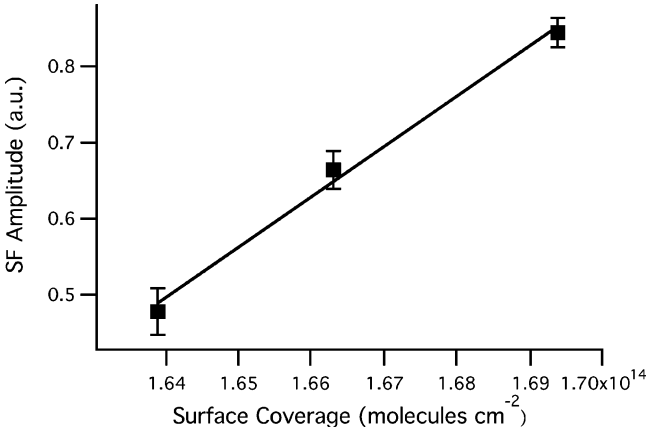

Figure 5. VSFS fit amplitudes of the C═O stretching vibration under ssp polarization as a function of surface excess for hexanoic acid at the air/water interface. The surface coverage for each bulk concentration was taken from surface tension data. The error bars are the standard deviations obtained from fitting multiple sets of VSFS data. The solid line is a linear fit to the data.

insight into the hydrogen bonding of the hexanoic acid headgroup with water at the aqueous interface. Infrared reflection adsorption spectroscopic (IRRAS) studies of long-chain fatty acid monolayers at the air/water interface show three features in the C═O stretching region at ∼1734−1739 cm^{-1}, ∼1715−1720 cm^{-1}, and ∼1700−1704 cm^{-1}.[24,25] These have been assigned to non-hydrogen-bonded, singly hydrogen-bonded, and doubly hydrogen-bonded carbonyl groups, respectively.[24,25] A comparison of these literature values to the VSFS hexanoic acid frequency at 1720 ± 2 cm^{-1} shows that the carbonyl group has a single hydrogen bond character with water at the air/water interface.

It is important to note that some ambiguity remains as to the nature of hydrogen bonding to the headgroup, since OH groups of both interfacial water molecules and neighboring acid molecules can potentially hydrogen bond to the carbonyl oxygen. Although bridging interactions between neighboring carboxyl headgroups are possible, it is unlikely to be the only type of bonding interaction to the C═O group. Further insight into the bonding interactions for hexanoic acid comes from our equilibrium surface tension measurements, which show that, at 5 mM hexanoic acid (bulk) concentration, the surface area per molecule is ∼59 $Å^2$. By comparison, estimates obtained from crystal structures give a carboxyl headgroup area for fatty acids of approximately 23−24 $Å^2$, much smaller than the surface area

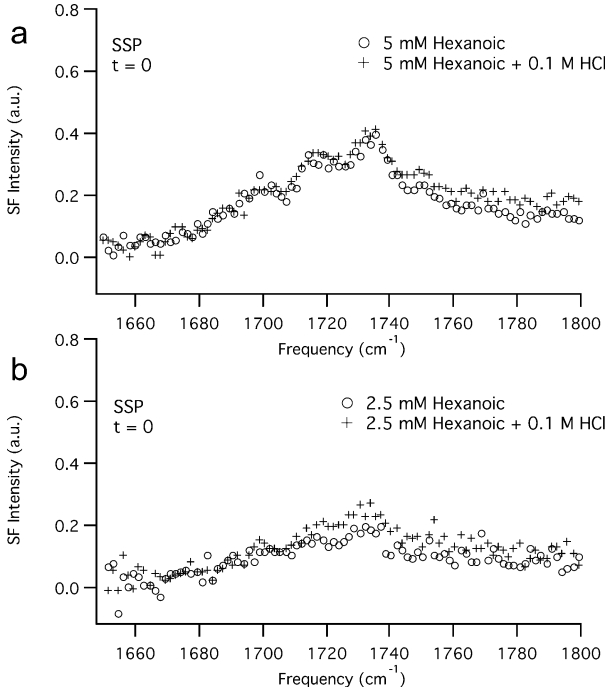

Figure 6. Comparison of $t = 0$ VSFS spectra under ssp polarization of the C═O stretching vibration of 5 mM (a) and 2.5 mM (b) hexanoic acid solutions with and without 0.1 M HCl.

demand for hexanoic acid.[26] This difference reflects the small interaction strength between adsorbed hexanoic acid molecules adsorbed at the air/water interface[21] and indicates that the hydrogen bonding interactions to hexanoic acid at the aqueous surface are mostly between the polar headgroup and the water.

In order to avoid adding extra ions, the pH of the solutions in Figure 4 has not been altered with a strong acid such as HCl. Given the hexanoic acid pK_a of 4.83 and the Nanopure water pH ∼ 6, it is conceivable that a sizable fraction (e.g., > 50%) of the neutral hexanoic acid headgroups at the surface could be ionized to the charged carboxylate form. Figure 6a compares VSFS spectra of the C═O stretching vibration in ssp polarization of 5 mM hexanoic acid solutions prepared with and without 0.1 M HCl. These spectra show that, although the pH of the 0.1 M HCl (pH ∼ 1) solution is well below the pK_a of hexanoic acid, the two spectra are not significantly different. Thus, the undissociated hexanoic acid, not the carboxylate form, is the dominant species at the 5 mM vapor−solution interface. Figure 6b shows a slight increase in the carbonyl intensity in the 2.5

TABLE 1: Average Resonant Widths and Amplitudes for the C═O Peak (1720 ± 2 cm^{-1}) Obtained from Hexanoic Acid Solution Spectra[a]

	$t = 0$		$t = 1.5$ h	
ssp polarization	Γ_ν	A_ν	Γ_ν	A_ν
5 mM	22 ± 2	0.84 ± 0.02	16 ± 2	1.75 ± 0.02
2.5 mM	22 ± 2	0.67 ± 0.02	16 ± 2	1.76 ± 0.02
1.5 mM	22 ± 2	0.48 ± 0.03	16 ± 2	1.78 ± 0.02
5 mM + NaCl	16 ± 2	1.33 ± 0.03	16 ± 2	1.33 ± 0.03
2.5 mM + NaCl	16 ± 2	1.22 ± 0.03	16 ± 2	1.48 ± 0.02
2.5 mM + Na_2SO_4	16 ± 2	1.34 ± 0.03	16 ± 2	1.58 ± 0.02
2.5 mM + NaCl/HCl	16 ± 2	1.53 ± 0.02	16 ± 2	1.50 ± 0.02
2.5 mM + Na_2SO_4/H_2SO_4	16 ± 2	1.62 ± 0.02	16 ± 2	1.61 ± 0.02
sps polarization	Γ_ν	A_ν	Γ_ν	A_ν
5 mM	23 ± 3	0.51 ± 0.03	10 ± 3	0.61 ± 0.03
2.5 mM	23 ± 3	0.38 ± 0.04	10 ± 3	0.60 ± 0.03
2.5 mM + NaCl	9 ± 3	0.71 ± 0.03	9 ± 3	0.72 ± 0.03
2.5 mM + Na_2SO_4	9 ± 3	0.80 ± 0.03	9 ± 3	0.80 ± 0.03
2.5 mM + NaCl/HCl	9 ± 3	0.71 ± 0.03	9 ± 3	0.71 ± 0.03

[a] All widths are given in units of cm^{-1}.

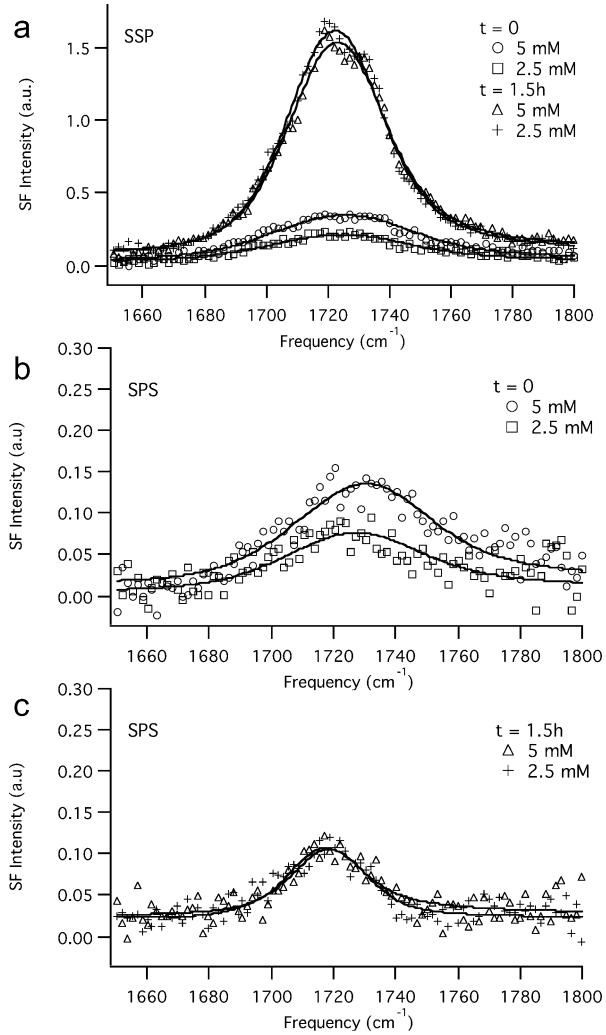

Figure 7. VSFS spectra of the C═O stretching vibration of 2.5 mM and 5 mM hexanoic acid solutions compared at $t = 0$ and $t = 1.5$ h taken under ssp polarization (a) and sps polarization (b,c). Solid lines are fits to the data.

mM hexanoic acid spectrum with 0.1 M HCl, which may be due to increased surface adsorption caused by a higher undissociated hexanoic acid concentration in the bulk. However, this increase is relatively small, suggesting that, at the 2.5 mM solution surface, the neutral acid species is preferentially adsorbed. This result is consistent with second harmonic generation spectroscopy studies probing the influence of the air/water interface on the acid−base equilibria of acids such as *p*-nitrophenol and bases such as *p*-hexadecyl aniline.[27,28] These studies show that, because of the higher free energy associated with surface adsorption of charged species, the acid−base equilibrium at the interface is shifted toward the energetically more favorable neutral aniline and phenol species.

To study the dynamics of hexanoic acid adsorption, the C═O group of the acid headgroup was monitored in time with VSFS. Spectra under ssp polarization are shown in Figure 7a of 1.5, 2.5, and 5 mM hexanoic acid solutions at the time intervals referenced as $t = 0$ and $t = 1.5$ h. The data were globally fit using C═O peak parameters obtained from the fits in Figure 4 and by holding the peak position at 1720 ± 2 cm^{-1} and the resonant phase constant across all of the spectra. Peak widths were allowed to vary between spectra at $t = 0$ and $t = 1.5$ h. Results of this analysis are shown in Table 1.

Spectral fitting confirms what is clearly evident in the data, that the C═O intensity significantly increases approximately

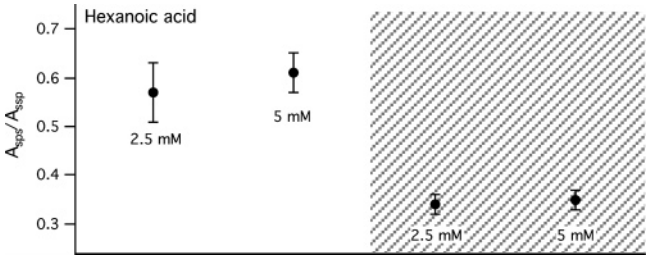

Figure 8. Trends in the ratio of fitted amplitudes, A_{sps}/A_{ssp}, for the C═O stretching vibration for 2.5 and 5 mM hexanoic acid aqueous solutions without salt. Amplitude ratios are compared at $t = 0$ (unshaded area) and $t = 1.5$ h after initial adsorption (shaded area). Error bars represent the uncertainty in the amplitudes.

1−1.5 h after the initial organic adsorption at the surface. As shown in Table 1, the spectral amplitude increases for the 1.5, 2.5, and 5 mM solutions. The C═O intensity is the lowest for the highest surface coverage at 5 mM bulk concentration. One interpretation of this spectral increase is continued hexanoic acid adsorption at the interface. However, our surface tension data show no change in the surface tension after 1−1.5 h, indicating no additional adsorption of hexanoic acid at the interface. As we observe, previous surface tension studies have shown that hexanoic acid adsorption at the surface reaches equilibrium quickly, on a time scale of milliseconds.[21]

Another interpretation for the spectral increases in Figure 7a is a slow reorientation of the C═O group. By examining hexanoic acid adsorption at the air/water interface under different polarization schemes, orientation changes may be deduced. Figure 7b,c shows the VSFS spectra under sps polarization for 5 mM and 2.5 mM hexanoic acid solutions at $t = 0$ and at $t = 1.5$ h. The spectra show none of the dramatic intensity increases observed in the ssp-polarization data; rather, there is a large change observed in the spectral profile. The frequency of the C═O mode at $t = 1.5$ h appears to be red-shifted and the bandwidth narrowed. The sps spectra were initially globally fit by constraining the C═O resonant phase to be equal for all four spectra but allowing the peak frequency and width to vary between the sets of spectra at $t = 0$ and $t = 1.5$ h. However, these constraints failed to produce adequate results. Much better fits to the data were achieved by holding the C═O frequency constant while allowing the peak phases and Gaussian widths to vary. These fits, shown in Figure 7b,c, reveal that the sps-polarization resonant response undergoes a phase shift and not a frequency shift after the initial adsorption of hexanoic acid at the aqueous surface. The same phase change is observed for both 2.5 and 5 mM concentrations. This analysis of the sps spectra also shows a small increase in the C═O resonant amplitude with time for the 5 mM and 2.5 mM spectra. These small amplitude increases are not revealed by visual inspection of the spectra because of the concurrent changes in peak phase and bandwidth.

By comparing the ratio of fit amplitudes, A_{sps}/A_{ssp}, at $t = 0$ and $t = 1.5$ h for the hexanoic acid solutions, the dependence on N, the surface molecular density is removed. The ratio then reflects the orientational characteristics of the surface. These amplitude ratios for 2.5 and 5 mM solutions change considerably over this time interval, as illustrated in Figure 8. This analysis, along with the time-dependent surface tension data, indicates that the increases in spectral amplitude in Figure 7 can be attributed to a change in the hexanoic headgroup average orientation with time. The shift in the C═O peak phase under sps polarization also supports a reorientation of the polar headgroup. As the headgroups reorient to achieve the most stable

surface configuration, it appears that molecules at the three surface coverages achieve a different orientation on average. If the final headgroup orientation is the same at 1.5, 2.5, and 5 mM, then one would expect the differences in spectral amplitude between the concentrations at $t = 1.5$ h to be greater and to scale with surface coverage as they do at $t = 0$, contrary to what we observe.

Concurrent with changes in spectral amplitude, the spectra in Figure 7 also show changes in the carbonyl bandwidth ~1.5 h after the initial organic adsorption at the surface. The C═O peak widths (fwhm) decrease in time for all concentrations, from 22 ± 2 cm^{-1} to 16 ± 2 cm^{-1} in ssp polarization and from 23 $\pm$ 3 cm^{-1} to 10 ± 3 cm^{-1} in sps polarization. In general, molecules experience a multitude of bonding environments at the aqueous interface, which affects their energy distribution and broadens the observed bandwidths beyond the fundamental line shape. This is particularly true for the OH stretching mode of water. For example, the broad and overlapping line shapes in the VSFS spectrum of the neat air/water interface are due to the wide variety of hydrogen-bonding environments experienced by water molecules.[29] Such bandwidth broadening also applies to the carbonyl mode, which is sensitive to changes in hydrogen bonding.[30−32] For example, in a study of aqueous mixtures of 1,2-dipalmitoylphosphatidylcholine (DPPC) and cholesterol, the decrease in C═O bandwidth with high hydrostatic pressure is due to a decrease in the ratio of hydrogen bonded to free carbonyl groups.[31] Carbonyl peak widths in the VSFS spectra of hexanoic acid solutions without salt are found to decrease as a function of time, indicating a reduction in the variety of hydrogen-bonding environments to the carboxyl headgroup. The results suggest that the observed headgroup reorientation that occurs at longer times is accompanied by an alteration of the solvation shell surrounding the polar headgroup. The bandwidth decrease is consistent with a reduction in the range of strengths of the H_2O−carbonyl bonding interaction and likely with more highly structured water solvating the headgroup at the surface.

As discussed above, the spectral changes to the C═O peak amplitude and phase are attributed to a reorientation of the polar group after initial adsorption at the surface. Thus, at the salt-free air/water interface, the spectral variations show slow changes to both the hexanoic acid headgroup average orientation and the solvation shell bonding structure with time. To the best of our knowledge, these two processes, reorientation and restructuring of the polar headgroup, that follow a fast surface adsorption of the organic acid have not been observed before.

Effect of Salts on Hexanoic Acid Surface Coverage. As illustrated by the surface tension results in Figure 3, the addition of NaCl and Na_2SO_4 to solutions of hexanoic acid enhances organic adsorption at the air/water interface. Compared with salt-free 2.5 and 5 mM hexanoic acid solutions, the organic surface concentration is ~34% higher in the presence of NaCl and ~20% greater in Na_2SO_4. Consequently, hexanoic acid molecules are more tightly packed at air/water interfaces of solutions containing chloride and sulfate salts, with decreases in molecular surface area of about 33% and 19%, respectively. For example, the surface area per molecule for hexanoic acid solutions is ~59 Å^2 at 5 mM and decreases to ~44 Å^2 with NaCl and ~49 Å^2 with Na_2SO_4. The surface area for hexanoic acid in the presence of salts, however, is still relatively large compared with size estimates for the carboxyl headgroup (~23 Å^2).[26] This indicates that, similar to hexanoic acid solutions without ions, the hydrogen bonding interactions in the presence of salts are primarily between the acid headgroup and the water molecules.

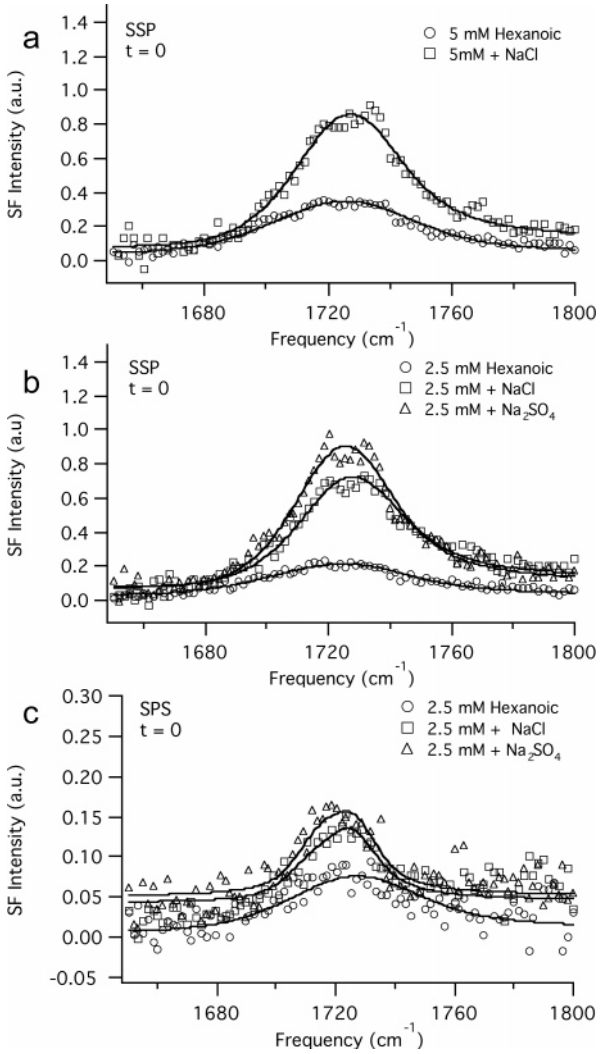

Figure 9. VSFS spectra of the C═O stretching vibration of the freshly prepared ($t = 0$) hexanoic acid−salt solution surface for (a) 5 mM hexanoic acid in 3 M NaCl under ssp polarization, (b) 2.5 mM hexanoic acid in 3 M NaCl and 1 M Na_2SO_4 under ssp polarization, and (c) 2.5 mM hexanoic acid in 3 M NaCl and 1 M Na_2SO_4 under sps polarization. The corresponding $t = 0$ spectrum of the salt-free hexanoic acid solution is shown with each figure for comparison. Solid lines are fits to the data.

The VSFS spectra at $t = 0$ of hexanoic acid solutions in Figure 9 are consistent with the effects of salts on organic surface adsorption found from thermodynamic measurements. Shown with the spectra are analytical fits obtained from global fitting with a single resonant feature, assigned to the C═O stretching mode, and a nonresonant background. The C═O feature is found at 1720 ± 2 cm^{-1}, unchanged from the peak frequency for hexanoic acid solutions without ions. This result verifies the conclusion drawn from the surface tension data, that headgroup bonding interactions are similar at hexanoic acid solution surfaces with and without ions.

The spectral fitting results in Table 1 show that the C═O intensity is greater upon initial organic adsorption in the presence of 3 M NaCl and 1 M Na_2SO_4, consistent with a salt-induced enhancement in organic adsorption at the aqueous interface. Compared with ssp spectra of hexanoic solutions without salt, the C═O amplitudes in Figure 9 are greater by ~55% for 5 mM hexanoic acid in NaCl, ~80% for the 2.5 mM NaCl solution, and ~100% for the 2.5 mM hexanoic−Na_2SO_4 solution. Table 1 also shows that the spectral amplitude is ~10% greater for the 2.5 mM hexanoic acid solution with sulfate than

with chloride. Figure 3, however, shows that the organic surface adsorption is higher in the presence of NaCl (~12%). This discrepancy between the spectral and the thermodynamic measurements could arise from differences in C═O group orientation at the surface in the presence of Cl^- versus SO_4^{2-} ions, to which only VSFS is sensitive.

In the VSFS and surface tension studies here, both Cl^- and SO_4^{2-} salts drive hexanoic acid molecules from the bulk to the air/water interface. This salt induced enhancement is consistent with the interfacial distributions of these anions. Molecular dynamics (MD) simulations and sum-frequency experiments show that sodium, sulfate, and chloride ions have somewhat different interfacial distributions: Cl^- is weakly adsorbed at the air/water interface, while Na^+ and SO_4^{2-} are strongly repelled from it.[33−37] Although chloride ions may reside in the interfacial region, these studies show that they are not found in significant excess at the surface relative to the bulk. Indeed, MD simulations predict that the Cl^- concentration in the top interfacial layer is ~30% below that in the bulk.[38] This suggests that the organic amphiphile may reduce the unfavorable energy costs of bulk solvation where the ion concentration is high by moving to the interface of NaCl and Na_2SO_4 solutions where the ion concentrations are much reduced.

Effects of Salts on Hexanoic Acid Headgroup Orientation. In addition to enhancing the hexanoic acid adsorption at the vapor/water interface, the presence of salts also measurably impacts the orientation dynamics of the hexanoic acid headgroup. We find that the ions induce a reorientation of the polar headgroup in the long time range following initial adsorption, as observed for the hexanoic acid solutions without ions. However, the most stable headgroup orientation at the surface differs between the salt-rich and the salt-free solutions. Furthermore, the orientation dynamics depend on the organic surface coverage, such that headgroup reorientation over time is not observed at high surface concentrations of hexanoic acid. This is in contrast to the behavior at the surface of hexanoic acid solutions without salts, where headgroup reorientation occurs for all concentrations examined. These orientation changes manifest in the VSFS spectra of the salt solutions as variations in the C═O intensity as a function of time.

Figure 10a shows that there is no significant change with time in C═O intensity for the 5 mM hexanoic acid solution with 3 M NaCl. This suggests that the headgroup orientation is invariant with time for the 5 mM hexanoic acid−salt solution, possibly because it reaches its optimum surface configuration immediately in the presence of ions because of high surface density and small surface area per molecule. By contrast, for the ssp spectra of 2.5 mM hexanoic acid solutions with NaCl and Na_2SO_4 in Figure 10b, the spectral intensity clearly increases in time at lower organic concentration. The addition of salts does not change the sps-polarization amplitudes for 2.5 mM hexanoic in 3 M NaCl in Figure 10c and in 1 M Na_2SO_4 solution (not shown). As shown in Figure 11a, the decrease in A_{sps}/A_{ssp} ratios indicates a reorientation of the headgroup over time for the 2.5 mM hexanoic acid−salt solutions.

This difference in headgroup orientation dynamics between salt solutions with 2.5 or 5 mM hexanoic acid is reasonable in light of the organic surface concentrations for these solutions. Upon initial organic adsorption at the surface of 2.5 and 5 mM hexanoic acid solutions with NaCl, the VSFS amplitude is approximately 10% greater for the 5 mM hexanoic−salt solution, consistent with surface coverage at these organic concentrations. However, at later times, this trend reverses so that the amplitude is greater for 2.5 mM hexanoic acid with

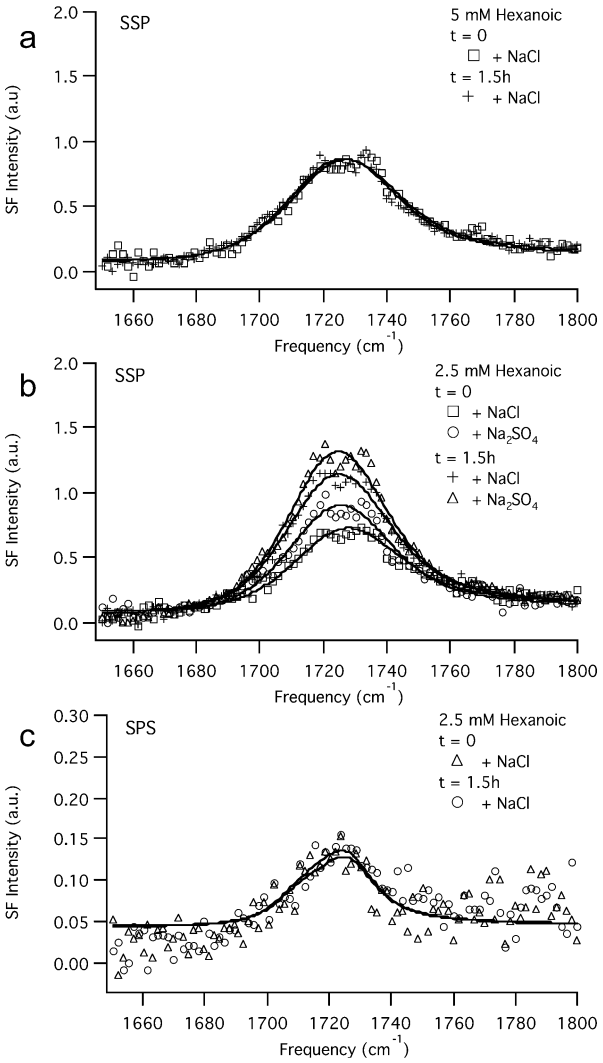

Figure 10. VSFS spectra in the C═O region of the freshly prepared ($t = 0$) hexanoic acid−salt solution surface compared with the salt solution surface after ~1.5 h of equilibration. Spectra under ssp polarization are shown for (a) 5 mM hexanoic acid in 3 M NaCl and (b) 2.5 mM hexanoic acid in 3 M NaCl and 1 M Na_2SO_4. Spectra under sps polarization are shown for (c) 2.5 mM hexanoic acid in 3 M NaCl. Solid lines are fits to the data.

NaCl, even though our measurements show that the organic surface coverage does not change over this time period. This indicates that the headgroups do not assume the same final orientation at the surface of 5 mM versus 2.5 mM hexanoic−salt solutions at the equilibrium surface configuration, likely because of differences in the organic surface area per molecule. The surface area is about 5% smaller for the 5 mM hexanoic acid−chloride solution than for 2.5 mM hexanoic acid with NaCl and may be small enough such that headgroup reorientation with time does not occur at the higher organic concentration.

We also find that the most stable headgroup orientation differs at the surface of hexanoic acid solutions with and without added salts. Figure 11b compares the A_{sps}/A_{ssp} ratios at the equilibrium surface configuration for 2.5 mM hexanoic solutions with and without NaCl and Na_2SO_4. The variation between these ratios shows that dissolved ions affect the final headgroup orientation at the vapor/water interface. Interestingly, however, the headgroup orientation is essentially the same upon initial adsorption of hexanoic acid at surfaces of salt-rich and salt-free solutions. This is illustrated in Figure 11c by the lack of variation between the $t = 0$ amplitude ratios for solutions with and without ions.

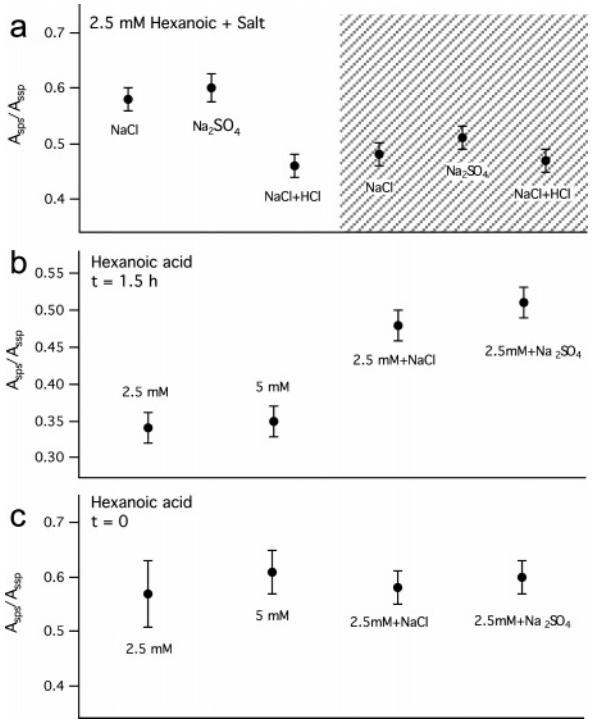

Figure 11. Trends in the ratio of fitted amplitudes (A_{sps}/A_{ssp}) for the C═O stretching vibration of hexanoic acid solutions. (a) Amplitude ratios for 2.5 mM hexanoic acid in NaCl, Na_2SO_4, and NaCl/HCl are compared at $t = 0$ (unshaded area) and $t = 1.5$ h after initial adsorption (shaded area). Amplitude ratios for hexanoic solutions with and without salt are compared in (b) at the equilibrium surface configuration ($t =$ 1.5 h) and in (c) upon initial adsorption ($t = 0$). The error bars represent the uncertainty in the amplitudes.

Effects of Salts on Hexanoic Acid Headgroup Bonding. We find that the addition of NaCl and Na_2SO_4 to the hexanoic acid solutions also affects the structure of the polar headgroup solvation shell. The dissolved ions perturb the headgroup environment possibly through ion−water interactions that increase the structure of solvating water molecules or that reduce the variety of water−headgroup interactions at the salt−solution surface. The salts are found to induce the most stable headgroup and water structure at the surface immediately upon hexanoic acid adsorption. This is in contrast to the salt-free solution, in which attaining the lowest energy configuration of hexanoic acid at the vapor/water interface involves a slow restructuring of the headgroup solvation shell. These ion effects on the water bonding around the organic headgroup are manifested in the VSFS spectra as changes to the C═O bandwidth.

The global fitting results in Table 1 show that the C═O peak widths are notably smaller upon initial adsorption ($t = 0$) for hexanoic acid at NaCl and Na_2SO_4 solution surfaces than those for the solutions without these salts. This bandwidth difference indicates that there is more homogeneity in the H_2O−carbonyl interactions and increased water structure in the headgroup solvation shell immediately upon adsorption for the ion containing solutions. The headgroup structure is not significantly different between the 2.5 and 5 mM hexanoic acid solutions with salts as evidenced by the similar C═O peak widths, suggesting similar ion−water interactions at the various organic concentrations. Furthermore, the salt solution C═O bandwidths do not narrow with time as they do at the surface of hexanoic acid solutions without ions, indicating that the equilibrium headgroup solvation structure is established much more quickly upon adsorption for the solutions with ions. Although added salts increase the rate at which the most stable water−carbonyl bonding interactions at the surface are achieved, they do not significantly alter the final bonding environment of the headgroup. This is demonstrated by the similarity in spectral bandwidths at $t = 1.5$ h between solutions with and without salts. Under both ssp and sps polarizations, the salt solution peak widths are the same within experimental error as the narrowed widths observed for hexanoic acid solutions without ions after 1−2 h of equilibration.

Effects of pH on Hexanoic Acid at the Surface of Ion Containing Solutions. Because the bulk solution pH should be different for NaCl and Na_2SO_4, additional VSFS experiments at low pH were conducted to separate ion effects from any salt-induced pH effects. As a result of these investigations, we find that pH differences between the two salt solutions do not contribute significantly to the ion specificity observed in the organic surface enhancement in Figure 9. Furthermore, unlike the 2.5 mM hexanoic acid−salt solutions without added protons, no significant change in the headgroup interfacial orientation with time is observed at low pH, as shown by the VSFS spectral intensities.

Hexanoic acid−salt solutions with the same ionic strength as those in Figure 9 were prepared by partially substituting salt with the corresponding acid, HCl or H_2SO_4. The strong acids were added at 0.1 M to give a solution pH well below the hexanoic acid pK_a that was about the same for both Cl^- and SO_4^{2-} containing solutions. Table 1 compares the ssp-spectral amplitudes at $t = 0$ for 2.5 mM hexanoic acid with those of NaCl/HCl and Na_2SO_4/H_2SO_4. The C═O amplitude at low pH is greater for the sulfate than for the chloride solution. In addition, the magnitude of this anion difference is the same within experimental uncertainty to that found in Figure 9 without the acid medium. This shows that salt-induced variations in solution pH do not play a significant role in the spectral intensity differences observed in Figure 9 between Cl^- and SO_4^{2-} containing hexanoic acid solutions.

Low pH spectra are shown as a function of time in Figure 12 for 5 mM hexanoic acid with NaCl/HCl and for 2.5 mM hexanoic acid with NaCl/HCl and Na_2SO_4/H_2SO_4. Global fitting results in Table 1 show that, at lower organic concentration (2.5 mM), greater acidity impacts the ssp-spectral intensities. In contrast to hexanoic−salt solutions without added acid, at low pH, the C═O amplitudes do not increase following initial adsorption. Figure 11a shows that the A_{sps}/A_{ssp} ratio is constant at low pH, suggesting that, unlike the 2.5 mM hexanoic acid−salt solutions without added protons, no significant change in the headgroup interfacial orientation with time is observed at low pH. This difference may be due to protonated water species at the organic−salt solution surface. Recent surface spectroscopic and theoretical studies indicate that, unlike other small cations, protons have a propensity for the water surface, and they may alter the orientation of surrounding water molecules.[35,39−41] Such species in close proximity to hexanoic acid molecules and their water of hydration at the interface could impact the dynamic structural changes of the polar headgroup.

As a result of these VSFS and surface tension studies, a general picture of hexanoic acid adsorption at vapor/water interfaces with and without added salts (NaCl and Na_2SO_4) emerges. Within the initial minutes, maximum surface coverage of hexanoic acid at aqueous surfaces with and without ions is complete. With time, there is a restructuring of the surfactants and surface water as they seek to achieve the lowest energy configuration. Both headgroup reorientation and changes in the water bonding around the headgroup occur as a function of adsorption time at the salt-free solution surface. The salts modify

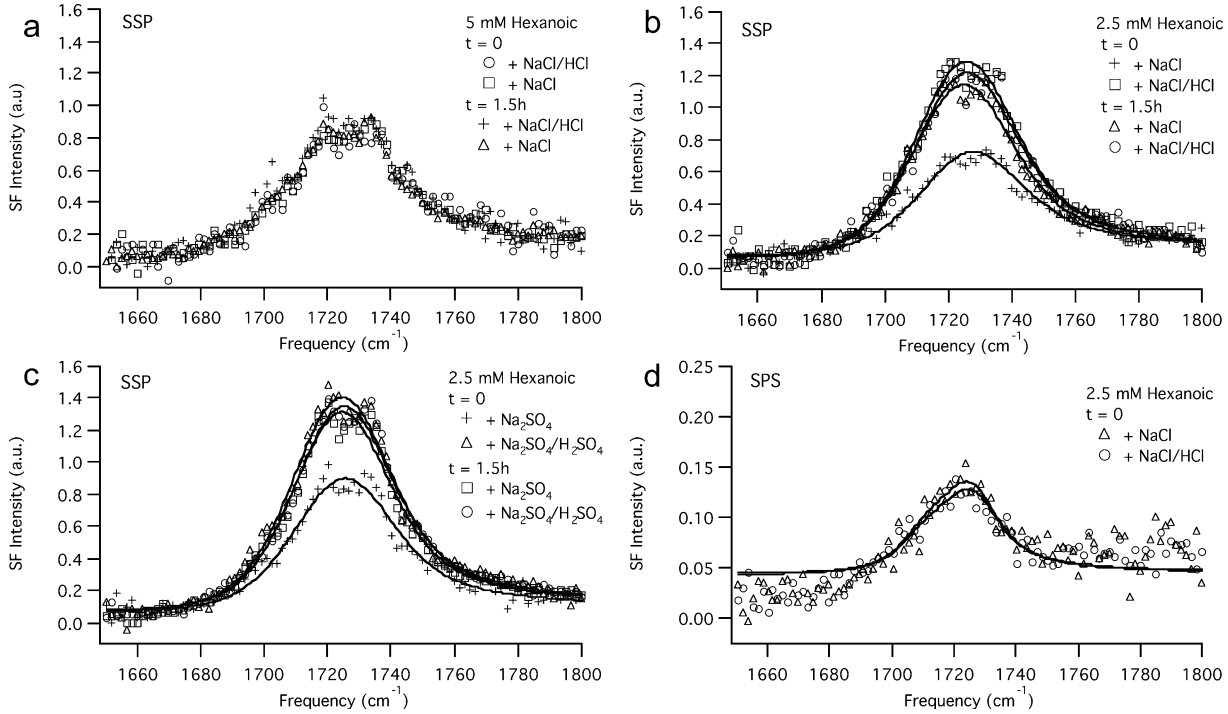

Figure 12. VSFS spectra in the C═O region of hexanoic acid−salt solutions at low pH compared with the same solutions without added protons. Surface spectra under ssp polarization of freshly prepared ($t = 0$) hexanoic acid−salt solutions are compared with those obtained after ∼1.5 h of equilibration for (a) 5 mM hexanoic acid solutions with 3 M NaCl/HCl, and for 2.5 mM hexanoic acid solutions with (b) 3 M NaCl/HCl and with (c) 1 M Na_2SO_4/H_2SO_4. Spectra under sps polarization at $t = 0$ are shown in (d) for 2.5 mM hexanoic acid in 3 M NaCl/HCl. Solid lines are fits to the data. Because the hexanoic−NaCl/HCl sps spectrum does not change in time, the sps spectrum at $t = 1.5$ h is not shown in (d) for clarity.

the adsorption of hexanoic acid at the aqueous interface by enhancing the organic surface coverage. In addition, the dissolved ions also influence the water−carbonyl interactions such that the most stable headgroup bonding environment is achieved immediately upon adsorption, in contrast to the solution without ions. With time at the surface of ion containing solutions, headgroup reorientation occurs but is dependent upon the organic surface coverage, with reorientation only observed at lower surface concentration.

4. Conclusions

Using vibrational sum-frequency spectroscopy and surface tensiometry, we have made measurements of the adsorption of hexanoic acid at the surface of electrolyte solutions to determine the effects of high ionic strength on organic adsorption at the vapor/aqueous interface of atmospheric aerosols. In the course of the studies, we have discovered that, for hexanoic acid at the vapor/water interface, the initial adsorption of the acid is followed by a reorientation and restructuring of the headgroup solvation shell after a period of 1−2 h. We find that both the initial adsorption and this headgroup reconfiguration are affected by the presence of ions. The surface tension data show that Na^+, Cl^-, and SO_4^{2-} ions abundant in aerosols enhance hexanoic acid adsorption at the aqueous interface. The spectroscopic studies provide molecular-level insight beyond this thermodynamic picture into the bonding and orientation of the organic headgroup at the salt solution surface. The addition of salts affects the solvation shell structure of the acid headgroup, such that upon initial adsorption, there are immediately fewer types of or more structured water−headgroup interactions for the ion containing solution than for the solution without ions. The bonding environment of the polar headgroup at the salt solution surface does not change as a function of time, in contrast to the restructuring observed with time in the absence of salts. Furthermore, we find that the polar headgroups slowly reorient at the aqueous interface of both salt-containing and salt-free solutions as they seek their lowest energy configuration but likely to a different average orientation with the added salts. However, the headgroup orientation is the same upon initial adsorption of hexanoic acid at the surface of solutions with and without ions.

Because aerosols are often a mixture of organic and inorganic components, these results have important implications for the adsorption of organic species to the aerosol surface and consequently for the surface reactivity of important atmospheric gases. For multicomponent aerosols, the surface concentration of organic species may be higher than predicted because of the presence of salts. In addition, because the presence of organics can affect the uptake of gaseous species at aerosol surfaces and their subsequent reactivity and diffusion into aerosol droplets, the results here of how ions modify the solvation and orientation of organic molecules at the air−water interface contributes to our understanding of atmospheric aerosol chemistry. In light of the growing awareness of the abundance of organic species in the atmosphere and their role in heterogeneous reaction processes, the present findings provide timely insight for elucidating how the adsorption of organics is affected by ions at an aqueous surface and how this might alter the physical and chemical properties of atmospheric aerosols.

Acknowledgment. The authors gratefully acknowledge the support of the National Science Foundation for this work (CHE-0652531).

References and Notes

(1) Cacace, M. G.; Landau, E. M.; Ramsden, J. J. *Q. Rev. Biophys.* **1997**, *30*, 241.

(2) Gilman, J. B.; Eliason, T. L.; Fast, A.; Vaida, V. *J. Colloid Interface Sci.* **2004**, *280*, 234.
(3) Cruz, C. N.; Pandis, S. N. *Environ. Sci. Technol.* **2000**, *34*, 4313.
(4) Rudich, Y. *Chem. Rev.* **2003**, *103*, 5097.
(5) Saxena, P.; Hildemann, L. M.; McMurry, P. H.; Seinfeld, J. H. *J. Geophys. Res.* **1995**, *100*, 18755.
(6) Russell, L. M.; Maria, S. F.; Myneni, S. C. B. *Geophys. Res. Lett.* **2002**, *29*.
(7) Saxena, P.; Hildemann, L. M. *J. Atmos. Chem.* **1996**, *24*, 57.
(8) Thornton, J. A.; Abbatt, J. P. D. *J. Phys. Chem. A* **2005**, *109*, 10004.
(9) Demou, E.; Donaldson, D. J. *J. Phys. Chem. A* **2002**, *106*, 982.
(10) Shen, Y. R. *The Principles of Nonlinear Optics*; John Wiley & Sons: New York, 1984.
(11) Richmond, G. L. *Chem. Rev.* **2002**, *102*, 2693.
(12) Eisenthal, K. B. *Chem. Rev.* **1996**, *96*, 1343.
(13) Shen, Y. R. *Nature* **1989**, *337*, 519.
(14) Kido-Soule, M. C.; Hore, D. K.; Jaramillo-Fellin, D. M.; Richmond, G. L. *J. Phys. Chem. B* **2006**, *110*, 16575.
(15) Bain, C. D.; Davies, P. B.; Ong, T. H.; Ward, R. N. *Langmuir* **1991**, *7*, 1563.
(16) Goates, S. R.; Schofield, D. A.; Bain, C. D. *Langmuir* **1999**, *15*, 1400.
(17) Moore, F. G.; Becraft, K. A.; Richmond, G. L. *Appl. Spectrosc.* **2002**, *56*, 1575.
(18) Rame, E. *J. Colloid Interface Sci.* **1997**, *185*, 245.
(19) Davies, J. T.; Rideal, E. K. *Interfacial Phenomena*; Academic Press: New York, 1961.
(20) Watry, M. R.; Richmond, G. L. *J. Am. Chem. Soc.* **2000**, *122*, 875.
(21) Li, B.; Geeraerts, G.; Joos, P. *Colloids Surf., A* **1994**, *88*, 251.
(22) Fainerman, V. B.; Zholob, S. A.; Miller, R.; Joos, P. *Colloids Surf., A* **1998**, *143*, 243.
(23) Rosen, M. J. *Surfactants and Interfacial Phenomena*; John Wiley & Sons: New York, 1978.
(24) Gericke, A.; Huhnerfuss, H. *J. Phys. Chem.* **1993**, *97*, 12899.
(25) Johann, R.; Vollhardt, D.; Moehwald, H. *Colloids Surf., A* **2001**, *182*, 311.
(26) Lunkenheimer, K.; Barzyk, W.; Hirte, R.; Rudert, R. *Langmuir* **2003**, *19*, 6140.
(27) Bhattacharyya, K.; Sitzmann, E. V.; Eisenthal, K. B. *J. Chem. Phys.* **1987**, *87*, 1442.
(28) Zhao, X.; Subrahmanyan, S.; Eisenthal, K. B. *Chem. Phys. Lett.* **1990**, *171*, 558.
(29) Raymond, E. A.; Tarbuck, T. L.; Brown, M. G.; Richmond, G. L. *J. Phys. Chem. B* **2003**, *107*, 546.
(30) Braban, C. F.; Carroll, M. F.; Styler, S. A.; Abbatt, J. P. D. *J. Phys. Chem. A* **2003**, *107*, 6594.
(31) Reis, O.; Winter, R.; Zerda, T. W. *Biochim. Biophys. Acta* **1996**, *1279*, 5.
(32) Nilsson, A.; Holmgren, A. *Proc. SPIE-Int. Soc. Opt. Eng.* **1992**, *1575*, 420.
(33) Jungwirth, P.; Curtis, J. E.; Tobias, D. J. *Chem. Phys. Lett.* **2003**, *367*, 704.
(34) Gopalakrishnan, S.; Jungwirth, P.; Tobias, D. J.; Allen, H. C. *J. Phys. Chem. B* **2005**, *109*, 8861.
(35) Tarbuck, T. L.; Richmond, G. L. *J. Am. Chem. Soc.* **2006**, *128*, 3256.
(36) Raymond, E. A.; Richmond, G. L. *J. Phys. Chem. B* **2004**, *108*, 5051.
(37) Jungwirth, P.; Tobias, D. *J. Phys. Chem. B* **2001**, *105*, 10468.
(38) Jungwirth, P.; Tobias, D. J. *J. Phys. Chem. B* **2002**, *106*, 6361.
(39) Petersen, M. K.; Iyengar, S. S.; Day, T. J. F.; Voth, G. A. *J. Phys. Chem. B* **2004**, *108*, 14804.
(40) Petersen, P. B.; Saykally, R. J. *J. Phys. Chem. B* **2005**, *109*, 7976.
(41) Tarbuck, T. L.; Ota, S. T.; Richmond, G. L. *J. Am. Chem. Soc.* **2006**, *128*, 14519.